Solid State Communications, Vol. 78, No. 9, pp. 835–839, 1991.
Printed in Great Britain.

0038–1098/91 $3.00 + .00
Pergamon Press plc

RESONANCE RAMAN SCATTERING OF $In_xAl_{1-x}As$ LATTICE MATCHED TO InP

N. Mestres[1], L. Viña[1,2], A. Manescau[3], E. Calleja[3], B. Koiller[4], P. Daste[5] and P. Riglet[5]

[1]Dpto. Física Aplicada, C-IV, Universidad Autónoma, Cantoblanco, E-28049 Madrid, Spain
[2]Instituto Ciencia de Materiales, CSIC, Cantoblanco, E-28049 Madrid, Spain
[3]ETSIT Universidad Politécnica, Ciudad Universitaria, E-28040 Madrid, Spain
[4]Dpto. de Física, PUC 22453 Río de Janeiro, Brazil
[5]L.E.P. Philips 94451 Limeil Brevannes, France

(*Received* 20 *December* 1990 *by F. Yndurain*)

We have studied MOCVD-grown $In_xAl_{1-x}As$ films, with x close to 0.52 (lattice matched to InP), by means of low temperature photoluminescence and Resonant Raman (RR) scattering. Besides the E_0 emission at ≈ 1.49 eV, we observe a weak photoluminescence band, B, ~ 50 meV above the fundamental one. In the Raman spectra, we identify the InAs-like and AlAs-like LO phonons and their overtones and combinations. An enhancement of the Raman efficiency for any of these phonons is observed at photon energies close to the B luminescence band. The resonance maximum red shifts with increasing In composition, according to the In-composition dependence of the E_0-gap. We suggest that the B luminescence originates from electronic transitions, due either to composition fluctuations through formation of macroscopic clusters or to the presence of resonant impurity states above the fundamental gap.

PRESENTLY, there is a strong interest in the ternary III–V semiconductor-alloy $In_xAl_{1-x}As$, due to its applications in electronic and optoelectronic devices. This is mainly because $In_xAl_{1-x}As$ can be lattice matched to InGaAs, InP or their alloys which have either high electron mobilities, high electron peak velocities or high electron saturation velocities. When these properties are combined with the high conduction band discontinuities of $In_xAl_{1-x}As$ with respect to these materials, $In_xAl_{1-x}As$-based heterostructures are amongst the best candidates for device applications in microwave, millimeter-wave and optoelectronic systems [1–4]. The emission wavelength of InGaAs/InAlAs quantum wells, lattice matched to InP, can be shifted from 1.65 μm to near 1.0 μm [5]. This spectral region spans the 1.3 μm minimum dispersion and 1.55 μm minimum loss regions of optical fibers.

Despite its importance, fundamental structural and electronic properties of $In_xAl_{1-x}As$, such as disorder in atomic arrangement and stress in this material, are still not fully clarified. In this paper, we present Resonant Raman (RR) scattering and photoluminescence (PL) results from $In_xAl_{1-x}As$ films, with x close to 0.52 (lattice matched to InP). The films were grown by metalorganic chemical vapor deposition (MOCVD) on [1 0 0] oriented InP substrates [6]. Pure hydrogen is used as carrier gas: the reaction occurs at 660°C in a horizontal reactor with a growth rate of 1 μm h^{-1}. The n-type residual carrier concentration is in the range of 1.2×10^{16} cm^{-3} with mobilities of about 3200 cm^2 V^{-1} s^{-1} at 300 K.

The total film thicknesses were ~ 1 μm, hence fully strain relaxed. Their fractional In content, x, was determined by X-ray diffractometry and also checked by photoluminescence and Raman scattering. Three samples with $x = 0.51$, 0.52 and 0.53 were investigated. They were mounted on a cold finger in an evacuated dewar and maintained in contact with liquid nitrogen. A jet-stream dye laser operated with LD700 (Spectra-Physics) was used to excite the samples. The dye was pumped with all the lines of a CW Kr^+ laser (4 W). We worked in the frequency range 1.57–1.77 eV, the power of the incident laser beam was typically between 20–40 mW. The scattered beam was analyzed by a Dilor XY triple-spectrometer equipped with an intensified cooled photodiode array detector, with a resolution of ~ 2 cm^{-1}. Pure silicon was chosen as a reference to normalize the scattering efficiency by the sample substitution method [7].

The Raman spectra were measured in backscattering geometry, $Z(X, X)\bar{Z}$, with X, Y and Z corresponding to the [1 0 0], [0 1 0] and [0 0 1] crystallographic directions, respectively. In this configura-

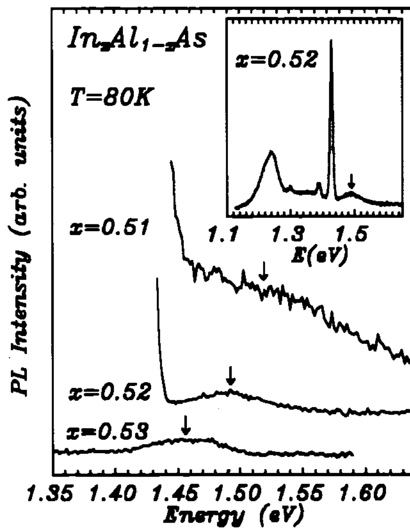

Fig. 1. Photoluminescence spectra of the $In_xAl_{1-x}As$ samples near the E_0-gap for three different In compositions. The energy of the E_0-gap is marked with an arrow. The inset depicts the recombination of the $In_{0.52}Al_{0.48}As$ sample in an extended spectral range, showing the below-band-gap recombination.

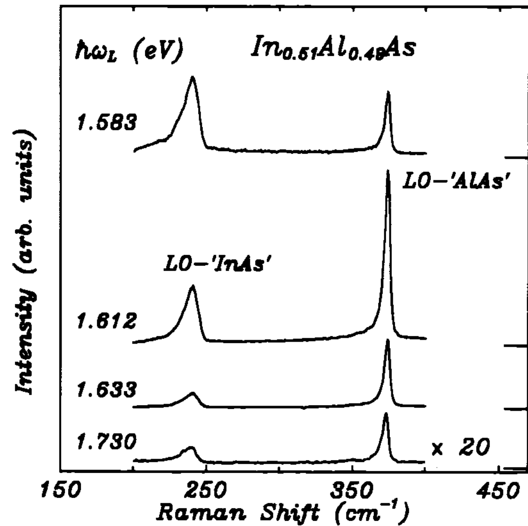

Fig. 2. Raman spectra of the $In_{0.51}Al_{0.49}As$ sample at different laser energies $\hbar\omega_L$. The peaks at ~ 240 and $\sim 374\,cm^{-1}$ correspond to the InAs-like and AlAs-like LO phonons, respectively. The resonant behavior of the AlAs-like LO phonon is clearly observed at energies closed to 1.61 eV. The measurements were performed at 80 K.

tion scattering by zone center longitudinal–optical (LO) phonons in a zinc-blend lattice is usually forbidden, according to the standard selection rules [7]. However, for laser energies near electronic transitions, in this configuration, scattering by LO phonons becomes allowed by the q-dependent, intraband Fröhlich and impurity induced electron-phonon, interaction mechanisms [7, 8].

The emission of our samples close to the fundamental band gap is depicted in Fig. 1. The 2.41 eV line of an Ar^+-laser was used to excite the samples. The inset shows the photoluminescence of the $In_{0.52}Al_{0.48}As$ sample in the 1.1–1.65 eV spectral range. The PL at 80 K is clearly dominated by impurities- and defects-associated recombination processes, below the band-to-band recombination (1.495 eV, marked with an arrow). A pronounced red shift with increasing In composition is observed in the spectra, which agrees with previously published data of the E_0-gap dependence on In concentration [9].

The Raman spectra of $In_xAl_{1-x}As$ display a two-mode type behavior, i.e. two LO modes associated with the respective end compounds are present for the whole composition range [10]. Figure 2 shows several Raman spectra from the $In_{0.51}Al_{0.49}As$ sample taken with different laser energies. All spectra have been normalized to those of pure silicon, which were measured simultaneously. The two peaks at $\hbar\omega_1 \approx 240\,cm^{-1}$ and $\hbar\omega_2 \approx 374\,cm^{-1}$ correspond to the InAs- and AlAs-like LO phonon modes, respectively [10]. The asymmetry of the peaks originates in the scattering by phonons with wavevectors $q \neq 0$ activated by the alloy disorder [11]. A resonant behavior of the AlAs-like LO phonon is clearly observed at energies close to 1.61 eV. The fact that the InAs-like LO phonon has still not reached resonance at this energy indicates that we are dealing with outgoing resonances [8], as it will be discussed later.

Photoluminescence measurements, when the samples are excited with laser radiation of frequency ~ 1.6 eV, reveal the existence of a new electronic transition, associated with a weak and broad (~ 75 meV) emission band (B). This near-resonance PL is shown in Fig. 3 for the three different samples. Note the presence of different phonon modes rising on the weak PL background. This emission, which does not shift with the laser energy, decreases rapidly in intensity as the exciting frequency is tuned away from the B-band; therefore, it was not observed in Fig. 1. This new electronic transition lies ~ 50 meV above the E_0-gap. These experiments also show a red shift of the B-band with increasing In composition, which roughly follows the In-composition dependence of the E_0 gap [9]. All samples show resonance enhancement of the AlAs-like and InAs-like LO phonon modes as the incident photon energy approaches the B-edge.

The electronic transition associated to the B-luminescence is responsible for the observed enhancement

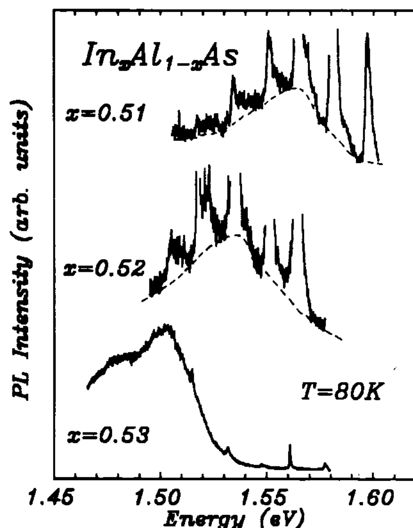

Fig. 3. Near resonance photoluminescence spectra for the three different samples. Note the red shift of the B luminescence band with increasing In composition. The sharp peaks correspond to InAs-like and AlAs-like LO phonons and their combinations.

in the Raman signal. Figure 4 compares the PL B-band with the AlAs-like LO phonon RR profile for the $In_{0.51}Al_{0.49}As$ sample. The Raman intensities are plotted as a function of the scattered photon energy, i.e. the resonant profile has been shifted to lower energies by the phonon frequency $\hbar\omega_2 = 46.6\,meV$.

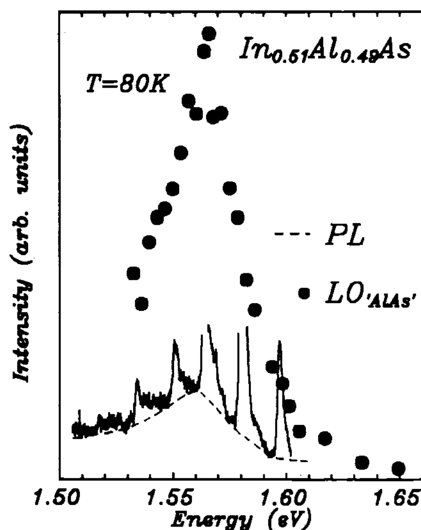

Fig. 4. Comparison of the B photoluminescence band with the AlAs-like LO phonon RR profile for the $In_{0.51}Al_{0.49}As$ sample. The resonance profile has been shifted to lower energies by the phonon energy ($\hbar\omega_2 = 46.4\,meV$). The fact that both curves coincide in energy position is consistent with an outgoing resonance.

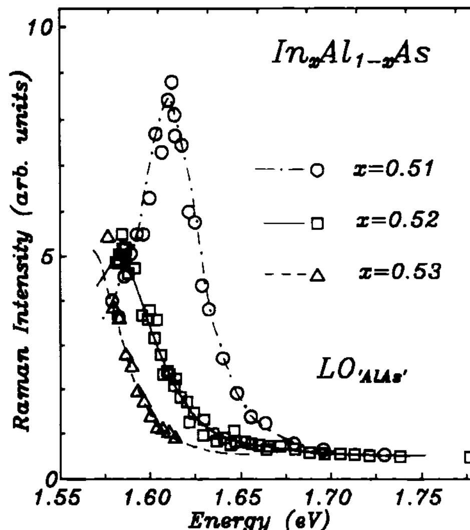

Fig. 5. Resonance Raman profiles of the AlAs-like LO phonon for the three samples of Fig. 1. The lines are drawn as a guide to the eye. A red shift of the resonance with increasing In composition is evident. Note that the energy range in the figure is above the E_0-gap of the alloys.

The fact that both curves coincide in energy position is consistent with an outgoing resonance. An outgoing resonance indicates that the impurity induced dipole-forbidden scattering mechanism is predominant, as expected for a material where structural defects and alloy disorder are important [8, 12].

Figure 5 depicts the AlAs-like LO phonon RR profiles, as a function of the incident laser energy in the available frequency range, for the three samples. The lines are drawn as a guide to the eye. A red shift of the resonance with increasing In content is evident, and agrees with the shifts observed in the near-resonance PL measurements. At the same time, a decrease of the Raman enhancement is observed with increasing In concentration. The systematic weakening of the LO resonance with increasing x is a result of increasing compositional disorder, which broadens the resonant structure, indicating shortening of the lifetime of the resonant state involved. This behavior is consistent with the broadening of the B-band photoluminescence as x increases (see Fig. 3).

Finally, we show in Fig. 6 a Raman spectrum of the $In_{0.52}Al_{0.48}As$ sample for an incident laser energy $\hbar\omega_L = 1.696\,eV$ in an extended energy range. Several overtones and up to five combinations of the InAs-like and AlAs-like LO phonon modes are clearly observed. A strong enhancement of the high-order Raman modes takes place only under extreme resonance conditions with direct interband transitions [7].

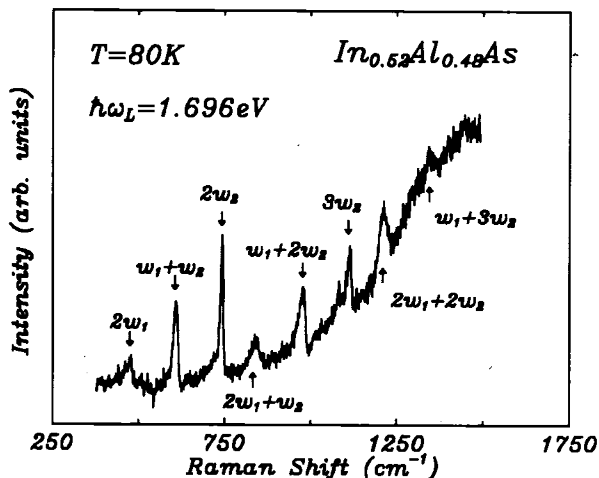

Fig. 6. Raman spectrum of the $In_{0.52}Al_{0.48}As$ sample. The arrows indicate the observed frequencies of the overtones on combinations of the InAs-like ($\hbar\omega_1$ = 241 cm^{-1}) and AlAs-like ($\hbar\omega_2$ = 372 cm^{-1}) LO phonon modes. The rise at high energies is due to photoluminescence.

Therefore, these results also indicate that an electronic transition above the fundamental E_0-gap ($\sim$ 1.495 eV) must be involved in the observed resonance effects.

From the luminescence and resonant Raman studies, we deduce the existence of a direct electronic transition slightly above ($\sim$ 50 meV) the fundamental E_0-gap. Following, we will like to focus our attention on the possible origin of this observed transition. The $In_xAl_{1-x}As$ system is expected to have a miscibility gap, due to the large difference between indium- and aluminium-related bond energies (114 and 140 Kcal mol^{-1}, respectively [13, 14]), and hence to show clustering. In fact, experiments based on photoluminescence and carrier transport indicate that MBE grown films are not of very high quality, and present alloy clustering [15–18]. In order to explain the observed electronic transition, we tentatively attribute it to local composition fluctuations. They can be induced by the random distribution of the In and Al cations in the sublattice of the $In_xAl_{1-x}As$ alloy. A supercell calculation in a tight binding framework [19], including up to 64 atoms, suggests that the B luminescence originates either from excited electronic transitions of a stochiometric configuration or from main transitions arising from clusters with small composition fluctuations. The experimental fact that the B luminescence is observed only in resonance conditions favors the latter theoretical interpretation.

However, an origin related to the presence of impurity states cannot be ruled out. Emission due to resonant impurity states above the conduction band minimum has been previously reported for $GaAs_{1-x}P_x$ alloys with isolelectronic traps [20].

In summary, we have observed electronic transitions slightly above the E_0-gap in MOCVD grown $In_xAl_{1-x}As$ alloys with $x \sim 0.52$ through resonant Raman scattering and near-resonance excitation photoluminescence. The peak position of these transitions red shifts with increasing In concentration, rigidly with the E_0-gap. These transitions have been tentatively assigned to composition fluctuations through formation of macroscopic clusters or to the presence of resonant impurity states above the fundamental gap.

Acknowledgements — We thank C. Tejedor for fruitful discussions. Part of this work was supported by the Spanish Ministry of Education under Grant Number MAT-88-0116-C02 and the Esprit basic research action Number 3180.

REFERENCES

1. C.L. Lin, P. Chu, A.L. Kellner, H.H. Wieder & E.A. Rezek, *Appl. Phys. Lett.* **49,** 1593 (1986).
2. L. Aina, M. Mattingly, A. Fathimulla, E.A. Martin, T. Loughran & L. Stecker, *J. Cryst. Growth* **93,** 911 (1988).
3. L.F. Palmateer, P.J. Tasker, W.J. Schaff, L.D. Nguyen & L.F. Eastman, *Appl. Phys. Lett.* **54,** 2139 (1989).
4. O. Wada, H. Nobuhara, M. Makiuchi, H. Hamaguchi, S. Sasa & T. Fujii, *J. Cryst. Growth* **95,** 378 (1989).
5. D.F. Welch, G.W. Wicks & L.F. Eastman, *Appl. Phys. Lett.* **43,** 762 (1983); H. Temkin, K. Alavi, W.R. Wagner, T.P. Pearsall & A.Y. Cho, *Appl. Phys. Lett.* **42,** 845 (1983).
6. J.N. Patillon, J.P. André, C. Jay, M. Iost, C. Delalande, B. Soucail & G.M. Martin, *Proceedings of the International Symposium on Physics of Semiconductors Applications 90*, August 20–21, Seoul (Korea), to be published.
7. M. Cardona, in *Light Scattering in Solids II,* Vol 50 of *Topics in Applied Physics*, (Edited by M. Cardona & G. Güntherodt), p. 19, Springer, Berlin (1982).
8. J. Menéndez & M. Cardona, *Phys. Rev.* **B31,** 3696 (1985).
9. B. Wakefield, M.A.G. Halliwell, T. Kerr, D.A. Andrews, G.J. Davies & D.R. Wood, *Appl. Phys. Lett.* **44,** 341 (1984).
10. S. Emura, T. Nakagawa, S. Gonda & S. Shimizu, *J. Appl. Phys.* **62,** 4632 (1987).
11. P. Parayanthal & F.H. Pollak, *Phys. Rev. Lett.* **52,** 1822 (1984).
12. W. Kauschke, M. Cardona & E. Bauser, *Phys. Rev.* **B35,** 8030 (1987).
13. G.B. Stringfellow, *J. Cryst. Growth* **65,** 454 (1983).

14. T.M. Brennan, J.Y. Tsao, B.E. Hammons, J.F. Klem & E.D. Jones, *J. Vac. Sci. Technol.* **B7,** 277 (1989).
15. K. Nakajima, T. Tanahashi & K. Akita, *Appl. Phys. Lett.* **41,** 194 (1982).
16. K.Y. Cheng, A.Y. Cho, T.J. Drummond & H. Morkoc, *Appl. Phys. Lett.* **40,** 147 (1982).
17. W.P. Hong, P.K. Bhattacharya & J. Singh, *Appl. Phys. Lett.* **50,** 618 (1987).
18. P. Chu, C.L. Lin & H.H. Wieder, *Appl. Phys. Lett.* **53,** 2423 (1988).
19. B. Koiller, M. Davidovich & L.M. Falicov, *Phys. Rev.* **B41,** 3670 (1990).
20. D.R. Scifres, N. Holonyak, C.B. Duke, G.G. Kleiman, A.B. Kunz, M.G. Caford, W.O. Groves & A.H. Herzog, *Phys. Rev. Lett.* **27,** 191 (1971).